Canadian Mineralogist
Vol. 30, pp. 613-631 (1992)

THE WODGINITE GROUP. II. CRYSTAL CHEMISTRY

T. SCOTT ERCIT[1], PETR ČERNÝ AND FRANK C. HAWTHORNE
Department of Geological Sciences, University of Manitoba, Winnipeg, Manitoba R3T 2N2

CATHERINE A. MCCAMMON[2]
Department of Physics, University of Manitoba, Winnipeg, Manitoba R3T 2N2

ABSTRACT

The wodginite group of minerals has been studied by electron microprobe, X-ray powder diffractometry, X-ray single-crystal methods, Mössbauer spectroscopy and atomic absorption spectroscopy. Ideal wodginite is $MnSnTa_2O_8$; however, wodginite also can host major amounts of Fe^{2+}, Fe^{3+}, Ti, Nb and Li, and minor to trace amounts of Sn^{2+}, Zr, Sc, W and Ca. Vacancies occur at the *A* (Mn) site and seem likely for the *B* (Sn) site. Three homovalent and four heterovalent mechanisms of substitution dominate wodginite chemistry, resulting in the four known species of the wodginite group plus synthetic $Mn_2Fe^{3+}Ta_5O_{16}$, which is not yet recognized as a natural species. A procedure for the calculation of formulae has been developed for electron-microprobe data; it permits calculation of Li contents and the Fe^{2+}:Fe^{3+} ratio. There is a strong correlation between structural and compositional properties of ordered members of the wodginite group. By multiple regression methods, a series of equations have been developed for the calculation of unit-cell parameters from compositional data for ordered members of the wodginite group; these equations give unit-cell parameters with root-mean-square errors averaging 0.007 Å on cell edges and 0.04° on the β angle. Natural members of the wodginite group are commonly partially disordered. The β angle, cell volume and the ratio $I(021)/I(220)$ are most sensitive to cation order. An index of order has been derived by comparing measured and calculated β angles, and it gives the degree of order to within 5%.

Keywords: wodginite group, order–disorder, crystal chemistry, tantalum.

SOMMAIRE

Nous avons étudié les minéraux du groupe de la wodginite par microsonde électronique, diffraction X (méthode des poudres et sur cristaux uniques), spectroscopie de Mössbauer et spectroscopie par absorption atomique. La formule idéale de la wodginite est $MnSnTa_2O_8$; toutefois, la wodginite accepte couramment des proportions importantes de Fe^{2+}, Fe^{3+}, Ti, Nb et Li, et des quantités moindres de Sn^{2+}, Zr, Sc, W et Ca. Des lacunes peuvent aussi impliquer la position *A* (Mn), et semblent probables dans la position *B* (Sn). Trois mécanismes de substitution homovalente et quatre de substitution hétérovalente régissent le champ de composition de la wodginite, et mènent aux quatre espèces connues dans ce groupe, en plus de $Mn_2Fe^{3+}Ta_5O_{16}$, qui n'a toujours pas été trouvé dans la nature. Nous décrivons un protocole de calcul de la formule pour les compositions déterminées à la microsonde électronique, afin d'obtenir la teneur en Li et le rapport Fe^{2+}:Fe^{3+}. Il existe une forte corrélation entre les propriétés structurales et compositionnelles des membres ordonnés du groupe de la wodginite. Nous nous sommes servis de régression multiple pour obtenir une série d'équations visant à calculer les paramètres réticulaires à partir de données sur la composition des membres ordonnés du groupe. Ces équations permettent de calculer les paramètres avec des erreurs de 0.007 Å et 0.04° sur les dimensions et l'angle β, respectivement. Les membres naturels de ce groupe montrent assez couramment un désordre partiel. L'angle β, le volume de la maille et le rapport $I(021)/I(220)$ sont les plus sensibles au degré d'ordre cationique. Un indice du degré d'ordre, bon à 5% près, découle de la différence dans les angles β mesuré et calculé.

(Traduit par la Rédaction)

Mots-clés: groupe de la wodginite, ordre–désordre, chimie cristalline, tantale.

[1]Present address: Mineral Sciences Section, Canadian Museum of Nature, Ottawa, Ontario K1P 6P4.
[2]Present address: Bayerisches Geoinstitut, Universität Bayreuth, Postfach 101251, 8580 Bayreuth, Germany.

INTRODUCTION

Work on the chemistry of wodginite has principally appeared in descriptive reports of its occurrence; there are few studies with the chemistry of the mineral as a primary objective. Given past confusion regarding the crystal structure of the mineral, its now recognized status as a group of minerals (Ercit *et al.* 1992a), its economic value as an ore mineral of tantalum, and its relatively common occurrence (Table 1), we decided to examine the crystal chemistry of the wodginite group.

Unlike studies of natural material, synthesis work has been directed toward understanding the crystal chemistry of the group. Turnock (1966) was the first to synthesize wodginite; he showed that ferric iron plays a role similar to that of tin in the structure. Komkov (1970) grew tin-bearing wodginite similar in chemistry to natural wodginite-group minerals. Sidorenko *et al.* (1974) showed that synthetic wodginite could be nonstoichiometric by growing samples with variable Sn:(Mn + Ta) ratios. Gatehouse *et al.* (1976) showed that Li could be incorporated into the wodginite structure in major amounts. Komkov & Dubik (1983) proved Sn ⇌ Ti isomorphism in synthetic wodginite.

Ferguson *et al.* (1976) showed the wodginite structure to be derived from an ixiolite substructure. Ixiolite is devoid of order of its cations; however, cations in the wodginite structure order into three distinct sites, causing a quadrupling of the unit-cell volume of the parent ixiolite subcell: $a_w = 2a_i$, $b_w = 2b_i$, $c_w = c_i$, where the subscripts w and i stand for wodginite and ixiolite, respectively. This scheme of cation order results in the ideal formula ABC_2O_8, with $Z = 4$ and space group $C2/c$; ideally A is populated by Mn, B, by Sn, and C by Ta (Ferguson *et al.* 1976). Owing to cation order, there are two chemically distinct types of zig-zag chains in the wodginite structure (Fig. 1). One type consists of alternations of A and B octahedra; the other consists solely of C octahedra. Only one type of chain occupies any given level in the closest-packed array; this results in two types of layers in the structure, one with chains of C polyhedra, the other with chains of A and B polyhedra. A more complete discussion of the structural crystallography of the wodginite group is given in Ercit *et al.* (1992b).

TABLE 1. LOCALITIES OF WODGINITE-GROUP MINERALS

Locality	Sample Obtained	Sample No.
1. Alto do Giz pegmatite, Brazil	Y	A-15
2. Ankole, Uganda	Y	A-17
3. Annie Claim pegmatite, Manitoba	Y	AC2-79, A-3
4. Benson pegmatite, Zimbabwe	N	
5. Coosa County, Alabama	Y	CX-1
6. Cross Lake, Manitoba	Y	CL-1
7. Erajarvi pegmatite field, Finland	N	
8. Greenbushes pegmatite, W. Australia	Y	GB-1 to -4
9. Herbb No. 2 pegmatite, Virginia	Y	H2-1
10. Kalbin Range, USSR	N	
11. Karibib, Namibia	Y	MC-1
12. Kazakhstan, USSR	Y	KZ-1
13. Red Cross Lake, Manitoba	N	
14. Kola Peninsula, USSR	Y	KO-1
15. Krasonice, Moravia, Czechoslovakia	Y	CZ-1
16. Lavra Jabuti, Minas Gerais, Brazil	Y	LJ-1 to -3
17. Marble Bar, W. Australia	Y	MB-1
18. Mt. Matthew, W. Australia	Y	MM-1
19. Muhembe River, Rwanda	Y	A-26
20. Nanping, China	Y	CH-1
21. Odd West pegmatite, Manitoba	Y	OW-102
22. Peerless pegmatite, S. Dakota	Y	A-29,-30
23. Eastern Sayan, USSR	N	
24. Seridozinho, Paraiba, Brazil	Y	BP-1
25. Eastern Siberia, USSR	N	
26. Strickland Quarry, Connecticut	Y	SQ-1
27. Kohero, Namibia	Y	OVK-8
28. Sukula pegmatite, Tammela, Finland	Y	SK-1
29. Tabba Tabba, W. Australia	Y	TT-1
30. Tahara, Japan	Y	TJ-1
31. Tanco pegmatite, Manitoba	Y	(G69-, SMP-, TSE-series)
32. Lower Tanco pegmatite, Manitoba	Y	
33. Tuscany, Italy	N	
34. Transbaikal region, USSR	Y	TB-1
35. Viitaniemi pegmatite, Finland	Y	VII-1
36. Wodgina, W. Australia	Y	WD-1
37. Yellowknife, NWT	Y	YKF-series

EXPERIMENTAL

Most of the electron-microprobe analyses were done at the University of Manitoba using energy dispersion (ED); the main data-set was augmented slightly with wavelength-dispersion (WD) data obtained at the Canadian Museum of Nature. ED X-ray spectra were obtained with a MAC 5 electron microprobe using a Kevex Micro-X 7000 spectrometer. Spectra were collected for 200 live seconds with an operating voltage of 15 kV and a sample current of 5 nA (measured on synthetic fayalite), and were corrected for current and voltage drift. Line overlaps, such as Ta$M\delta$ and Ta$M\eta$ on Nb$L\alpha$, Sn$L\beta$ on Ti$K\alpha$, and Mn$K\beta$ on Fe$K\alpha$ were dealt with by non-iterative techniques of spectral stripping involving library spectra of individual elements taken from standards used in the analysis of wodginite. Manganotantalite (Mn$K\alpha$, Ta$M\alpha$), fayalite and chromite (Fe$K\alpha$), rutile and titanite (Ti$K\alpha$), cassiterite (Sn$L\alpha$), $CaNb_2O_6$ (Nb$L\alpha$), Sc metal (Sc$K\alpha$), ZrO_2 (Zr$L\alpha$) and microlite (Ca$K\alpha$) were used as standards. Data were reduced with Kevex software using the MAGIC V program (Colby 1980). WD X-ray analyses were done with a JEOL 733 electron microprobe using Tracor Northern 5500 and 5600 automation. The operating potential was 15 kV; a 25 nA beam current was used. Data for standards were collected for 25 s or 0.25% precision per element, whichever was attained first. Data for samples were collected for 50 s or 0.5% precision at the 1σ level, whichever was attained first. The following standards were used: $NiTa_2O_6$ (Ta$M\alpha$), $MnNb_2O_6$ (Mn$K\alpha$, Nb$L\alpha$), cassiterite (Sn$L\alpha$), rutile (Ti$K\alpha$), almandine (Fe$K\alpha$), *REE*-bearing

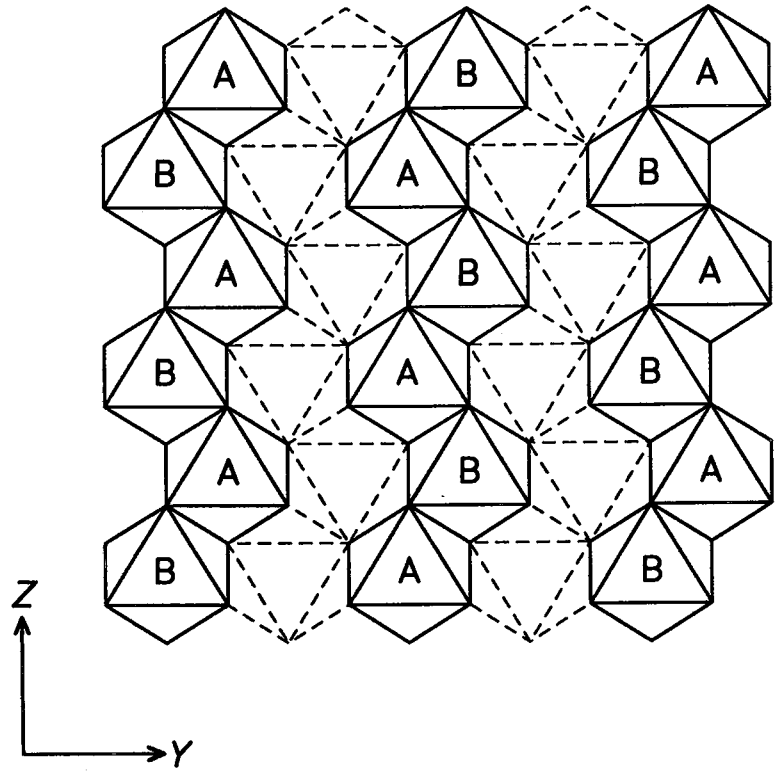

FIG. 1. The ideal structure of wodginite projected along *X*. Polyhedra of one level along *X* are shown in solid rule; polyhedra of adjacent levels are shown in broken rule. *A* and *B* octahedra occupy one level of the structure; their pattern of order is shown. *C* cations occupy the octahedra shown in broken rule. The octahedra share *cis*-edges along *Z*, which produces α-PbO_2-like zig-zag chains.

glass (Sc$K\alpha$), $CoWO_4$ (W$M\alpha$) and synthetic ZrO_2 (Zr$L\alpha$). Overlap between W$M\alpha$ and Ta$M\beta$ was manually corrected prior to data reduction. Data reduction was done with a conventional ZAF routine in the Tracor Northern TASK series of programs. Lithium determinations were done by atomic absorption spectroscopy by Mr. V. Kubat of the Ecole Polytechnique. 57Fe Mössbauer spectra were collected at the University of Manitoba. Samples were powdered and were mixed with benzophenone to ensure random orientation of the grains. Because of their high Ta contents, wodginite-group minerals are strong γ-ray absorbers; the optimum sample thickness was calculated according to the procedure of Long *et al.* (1983). Spectra were obtained at room temperature, collected with a 512-register multichannel analyzer, and were folded to give 245 data points over an approximate range of −4 to +4 mm/s (relative to α-Fe foil).

Philips PW1050 and PW1710 powder diffractometers were used to collect the powder-diffraction data, except for a few, very small samples, for which either a conventional 114.6-mm-diameter Gandolfi camera or a Nicolet R3m single-crystal diffractometer was used. For powder diffractometry, Ni-filtered or monochromated Cu$K\alpha$ radiation was used; annealed CaF_2 [a = 5.46379(4) Å] was the internal standard. Indexing and refinement of unit-cell parameters were done with the CELREF program of Appleman & Evans (1973). Weights were assigned to each measurement according to the following scheme. Sharp peaks of normal width at half height were assigned weights of 1; all ragged or abnormally broad peaks were assigned weights of 0.1 to 0.5, depending upon the quality of the peak. Peaks that were obviously in an overlapping relationship were omitted from the refinement.

Most heating experiments were done in air with a Fisher Isotemp muffle furnace, Model 186. The furnace temperature was periodically calibrated by monitoring the melting point of NaCl. Temperature regulation by the furnace is precise to ± 20°C.

Some heatings were done in controlled ($CO:CO_2$) atmospheres with a vertical quench furnace; temperature control with this furnace is precise to ± 10°C. Mineral syntheses were done anhydrously at atmospheric pressures using the Fisher muffle furnace. Reagent-grade pure oxides and carbonates were used as starting materials. Starting powders were weighed to produce 0.3 to 0.5 g samples, and were mixed by light hand-grinding in acetone for 20 minutes. The mixed powders were then pressed into pellets under a 10000 kPa load to optimize reactivity. After 4 to 10 hours of heating, samples were removed from the furnace, reground, and subjected to continued heating. In most cases, reactions were complete after 4 to 20 hours; however, some samples required repeated grinding and heating (up to 40 hours). For both the heating and synthesis experiments, Ag–Pd foil was used as a sample holder for runs at 1050°C or lower; Pt foil was used in all runs at higher temperatures, and some runs at 1000°C. The foil was iron-soaked where necessary.

CHEMISTRY

Results of electron-microprobe analyses

Results of electron-microprobe analyses of selected wodginite-group minerals are given in Table 2; other results can be found in Ercit *et al.* (1992a,b), and a tabulation of all 214 compositions obtained for the present study is available from the Depository of Unpublished Data, CISTI, National Research Council of Canada, Ottawa, Ontario K1A 0S2.

TABLE 2. CHEMICAL COMPOSITION OF SELECTED WODGINITE-GROUP MINERALS

	A-3	A-26	CH-1	KO-2	KZ-1	MC-1	TJ-1	TSE-16
Li_2O, wt.%	0.00	0.20	0.17	0.00	0.35	0.00	0.00	0.14
MnO	10.7	4.3	9.0	9.9	7.1	11.0	9.6	8.9
FeO	0.0	6.3	1.3	0.0	0.0	0.0	1.6	2.3
Sc_2O_3	0.0	0.0	0.0	0.0	0.0	0.0	1.7	0.0
Fe_2O_3	1.1	1.7	2.0	0.0	0.0	0.0	0.1	1.2
TiO_2	0.2	0.9	0.1	0.0	0.0	0.0	4.7	5.5
ZrO_2	0.0	0.0	0.0	0.0	0.0	0.0	0.2	0.0
SnO_2	15.8	14.5	14.0	17.8	7.8	14.5	7.4	8.8
Nb_2O_5	6.6	10.9	5.9	4.3	10.8	4.4	0.8	11.1
Ta_2O_5	64.6	61.1	67.0	66.3	73.7	68.9	71.0	60.4
WO_3	---	---	---	---	---	---	0.6	---
	99.1	99.9	99.6	98.4	99.7	98.8	97.8	98.3
				Cations per 32(O)				
Li	0.00	0.32	0.28	0.00	0.61	0.00	0.00	0.23
Mn	3.28	1.51	3.27	3.71	2.54	4.08	3.48	3.01
Fe^{2+}	0.44	2.17	0.45	0.00	0.00	0.00	0.56	0.76
Sc	0.00	0.00	0.00	0.00	0.00	0.00	0.62	0.00
Fe^{3+}	0.61	0.51	0.64	0.00	0.00	0.00	0.05	0.35
Ti	0.04	0.29	0.05	0.00	0.00	0.00	1.52	1.67
Zr	0.00	0.00	0.00	0.00	0.00	0.00	0.05	0.00
Sn	2.45	2.36	2.39	3.14	1.32	2.55	1.26	1.40
Nb	1.09	2.02	1.14	0.85	2.07	0.88	0.15	2.01
Ta	7.81	6.82	7.78	7.96	8.54	8.25	8.28	6.57
W	---	---	---	---	---	---	0.07	---
	16.00	16.00	16.00	15.65	15.07	15.89	16.05	15.95

- $Fe^{2+}:Fe^{3+}$ and Li_2O are calculated according to stoichiometric constraints (see text), except for sample KZ-1 (Li_2O measured).
- data for samples CH-1, KZ-1 and TJ-1 are averages of two analyses each.
- "0": not detected, "---": not measured

TABLE 3. VARIATIONS IN CHEMISTRY OF THE MAJOR ELEMENTS

Element	Mean	Maximum	Minimum	Ideal
Mn	7.1	9.1	2.1	8.3
Fe	1.7	8.7	0.0	0.0
Ti	1.4	6.2	0.0	0.0
Sn	9.7	15.1	0.5	17.9
Nb	4.0	11.7	0.5	0.0
Ta	54.9	75.5	43.6	54.5

All figures refer to wt. % of the element

Ferguson *et al.* (1976) gave the ideal formula of wodginite as $MnSnTa_2O_8$; as the data in Table 2 attest, wodginite strays far from ideality. The main substituents for Mn, Sn^{4+} and Ta are Fe, Ti and Nb; trace amounts of Sn^{2+} (E.E. Foord, pers. comm.), Zr, Sc, Ca, and W have been detected, and Li can be present. Maximum variations for each element are summarized in Table 3.

Cation–cation correlation plots (Fig. 2) attest to some of the dominant mechanisms of substitution for wodginite-group minerals. Figure 2a is a plot of total Fe *versus* Mn. The strong, linear correlation between total Fe and Mn ($R = -0.85$), with a slope of -1, indicates that most Fe in wodginite-group minerals is incorporated by Fe-for-Mn substitution; this also suggests that the ferrous state of Fe is the dominant one. However, several of the data points fall off the main trend, particularly at very low Fe contents. This finding indicates that significant mechanisms of substitution not involving Fe also operate at the *A* site.

A good negative correlation exists between Ti and Sn (Fig. 2b); however, only 52% of the variation in Sn can be accounted for by Ti-for-Sn substitution. Figure 2b shows that substantial Ti-for-Sn substitution is possible in natural members of the wodginite group: some samples show up to 75% of their Sn replaced by Ti. Despite the linear trend, all data points are displaced below the ideal curve for Sn ⇌ Ti isomorphism (bold line in Fig. 2b), showing that constituents other than Sn and Ti occur at the *B* site. The deviation of the data points from the trend increases as the Ti content decreases; some samples with no detectable Ti deviate from ideality by almost 100%.

Ta ⇌ Nb isomorphism is extensive (Fig. 2c); wodginite-group minerals show Nb:Ta as high as 0.35, although the norm is much lower. Ideal wodginite should have a maximum of 8(Ta + Nb) per unit cell; however, as Figure 2c shows, this number is always significantly exceeded, with a maximum deviation of 3.7 *surplus* (Ta + Nb) cations per unit cell, and a mean deviation in the vicinity of 1 cation per unit cell. The samples with Ta + Nb greatly in excess of 8 cations per unit cell correspond to data points that deviate significantly from ideal Sn ⇌ Ti isomorphism (Fig. 2b), indicating that excess Ta or Nb is incorporated at the *B* site, as shown in the structure analysis of Ferguson *et al.* (1976). Figure 3 shows that it is

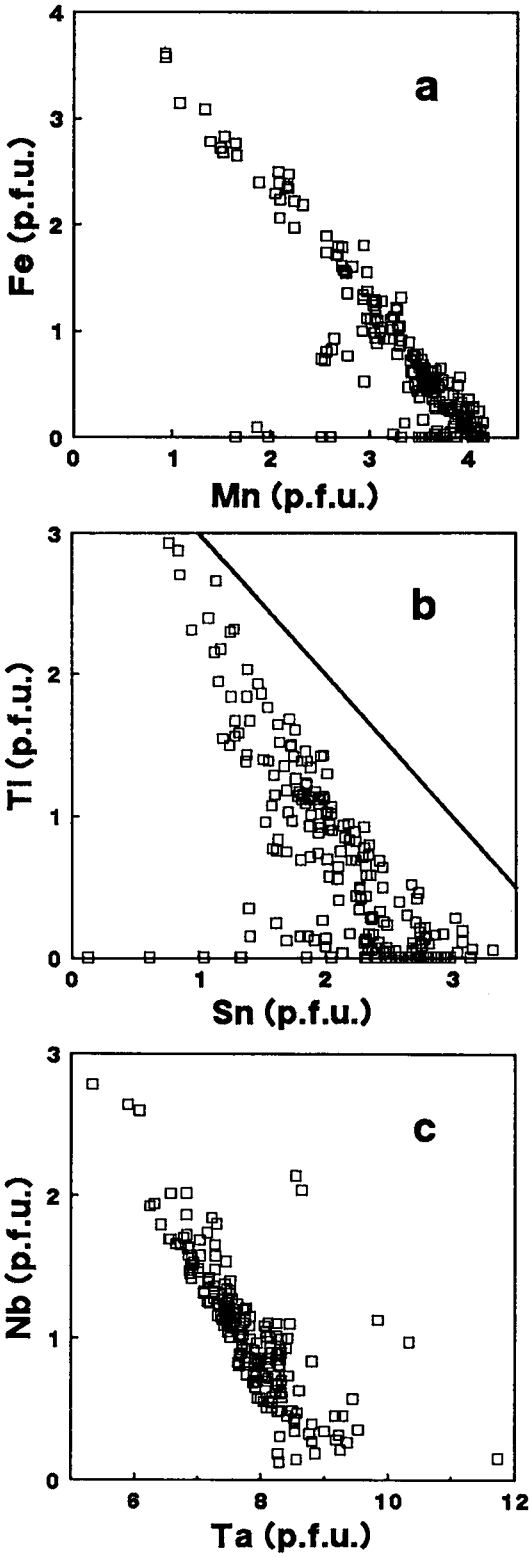

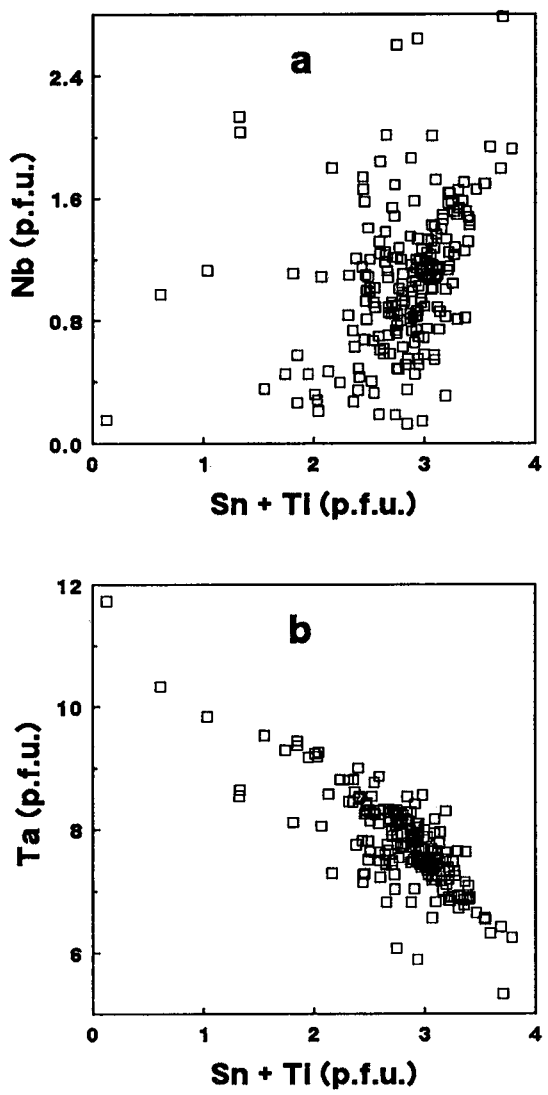

FIG. 3. Relationships between M^{5+} and M^{4+} cations. (a) Nb *versus* M^{4+} cations; (b) excess Ta (= *B*-site Ta) *versus* M^{4+} cations. The lack of any (negative) correlation between Nb and M^{4+}, and the presence of a good negative correlation between Ta and M^{4+}, show that Nb is not involved in *B*-site chemistry.

FIG. 2. Plots of cation–cation correlations plots: (a) total Fe *versus* Mn; (b) Ti *versus* Sn (the line shows the ideal 1:1 slope); (c) Ta *versus* Nb.

only excess Ta and not Nb that is incorporated at the *B* site. It is interesting to note that to date, wodginite has the only known structure for which Nb and Ta show differences in ordering behavior.

Mössbauer spectroscopy

Although preliminary cation–cation plots suggest that much of the Fe in wodginite-group minerals is ferrous and resides at the *A* site (Fig. 2a), the evidence is indirect; consequently, direct examination of the valence of iron in wodginite-group minerals was done by Mössbauer spectroscopy. Measurements were made on seven samples; five of these are naturally occurring members of the wodginite group, including the inferred Fe^{2+}-rich sample A–17 from Ankole, Uganda, and two are synthetic Fe^{3+}-rich samples that fall close to $Mn(Fe^{3+}Ta)Ta_2O_8$ in composition (synthesized by Turnock 1966).

The ^{57}Fe Mössbauer spectra are shown in Figure 4. The synthetic samples (TR1–1 and TR3–1) are characterized by a single absorption doublet, with an isomer shift of about 0.4 mm/s, and a quadrupole splitting of 0.5 mm/s. This is undoubtedly due to Fe^{3+}; the absence of any other doublets in these spectra confirms that all the iron is ferric, as Turnock (1966) inferred from the $f(O_2)$ conditions of the synthesis.

All naturally occurring members of the wodginite group have ^{57}Fe Mössbauer spectra that differ from those of the synthetic samples. The absorption envelope near the Fe^{3+} doublet is more complex, and there is a substantial additional component with an absorption maximum at approximately 2 mm/s. Both features are consistent with a doublet having an isomer shift of about 1.1 mm/s and a quadrupole splitting of about 2 mm/s, characteristic of Fe^{2+}.

Individual ^{57}Fe Mössbauer parameters and Fe^{2+}:Fe^{3+} ratios are given in Table 4; compositional information for the samples used in the Mössbauer experiments is given in Table 5. For the natural iron-rich samples studied here, the proportion of Fe^{2+} varies from 68% to 83% of the total Fe. This finding indicates that natural wodginite-group minerals as a whole show variable valences of iron, but confirms that they tend to have Fe^{2+} dominant over Fe^{3+}. The fact that the Sn-free wodginite samples synthesized by Turnock (1966) are unstable at low $f(O_2)$ indicates that Fe^{2+} cannot be stabilized at the *B* site of ordered wodginite. This finding implies strong order of Fe^{2+} at the *A* site and Fe^{3+} at the *B* site.

E.E. Foord (pers. comm.) has carried out a ^{119}Sn experiment on wodginite CX–1 from Coosa County, Alabama. A very small proportion of the tin in the sample is divalent (7 ± 3%), and most probably substitutes for Mn in the structure, on the basis of its charge and inferred size (effective ionic radius of $^{VI}[Sn^{2+}]$ = 1.10 Å from calculations by the authors). Sn^{2+} is scarce in the high-$f(O_2)$ environments in which wodginite-group minerals occur, as indicated by the common association of wodginite and cassiterite, and very rare association of wodginite and stannomicrolite (Ercit *et al.* 1987). Consequently, Sn^{2+} contents of all natural members of the wodginite group are expected to be extremely low, and in this study, all Sn determined by microprobe is assumed to be tetravalent.

TABLE 5. COMPOSITIONAL DATA (wt.%) FOR WODGINITE SAMPLES USED IN MÖSSBAUER EXPERIMENTS

	A-17		GB-2	GB-4	LJ-2		TSE-126	
	core	rim			core	rim	core	rim
MnO	5.4	4.7	6.4	6.2	7.5	7.1	10.2	10.0
FeO	5.8	6.4	4.7	4.6	3.6	3.7	1.5	1.5
Fe_2O_3	1.3	1.5	1.6	1.8	1.3	1.4	0.8	0.8
TiO_2	2.2	3.3	0.7	1.4	0.0	0.0	7.7	4.6
SnO_2	11.0	10.4	14.6	13.2	15.3	15.6	7.9	10.6
Nb_2O_5	7.5	8.0	6.3	5.6	6.9	7.2	9.5	7.9
Ta_2O_5	66.9	64.8	64.5	66.5	65.0	64.2	61.1	62.6
	100.1	99.0	98.8	99.4	99.8	99.2	98.6	98.0
	Cations per 32(O)							
Mn	1.89	1.66	2.33	2.24	2.69	2.57	3.42	3.49
Fe^{2+}	2.01	2.22	1.69	1.65	1.30	1.31	0.49	0.53
Fe^{3+}	0.41	0.45	0.51	0.58	0.43	0.43	0.23	0.25
Ti	0.69	1.03	0.23	0.44	0.00	0.00	2.29	1.42
Sn	1.82	1.71	2.49	2.24	2.61	2.66	1.25	1.75
Nb	1.41	1.49	1.21	1.08	1.32	1.39	1.69	1.47
Ta	7.57	7.30	7.50	7.68	7.54	7.47	6.57	7.03
	15.81	15.85	15.96	15.90	15.89	15.84	15.95	15.95

- Fe^{2+}:Fe^{3+} estimated from Mössbauer spectra; formula calculations were done ignoring the possibility of Li.

TABLE 4. ^{57}Fe MÖSSBAUER PARAMETERS

Sample	Fe^{2+}			Fe^{3+}			$\frac{Fe^{3+}}{Fe}$
	Γ	δ**	ΔEq	Γ	δ**	ΔEq	
A-17	0.66(7)	1.08(13)	2.16(7)	0.32(8)	0.37(4)	0.15(11)	0.17(7)
GB-2	0.57(6)	1.09(4)	2.05(7)	0.33(5)	0.42(4)	0.17(10)	0.26(3)
GB-4	0.54(6)	1.10(4)	1.92(7)	0.27(12)	0.47(4)	0.18(9)	0.23(4)
LJ-2	0.64(11)	1.06(14)	2.05(25)	0.34(46)	0.38(11)	0.15(78)	0.25(7)
TSE-126	0.58(15)	1.16(6)	1.94(17)	0.44(15)	0.15(13)	0.54(24)	0.32(9)
TR1-1	----	----	----	0.52(6)	0.37(4)	0.53(6)	1.0
TR3-1	----	----	----	0.49(5)	0.39(5)	0.54(6)	1.0

- all units are mm/s, ** relative to Fe-foil

Lithium determinations

In their study of the polymorphs of $LiTa_3O_8$, Gatehouse *et al.* (1976) found that the medium-temperature polymorph, *M*-$LiTa_3O_8$, has the wodginite structure. Voloshin *et al.* (1990) found the first natural occurrence of this compound, and

FIG. 4. ^{57}Fe-Mössbauer spectra of wodginite-group minerals.

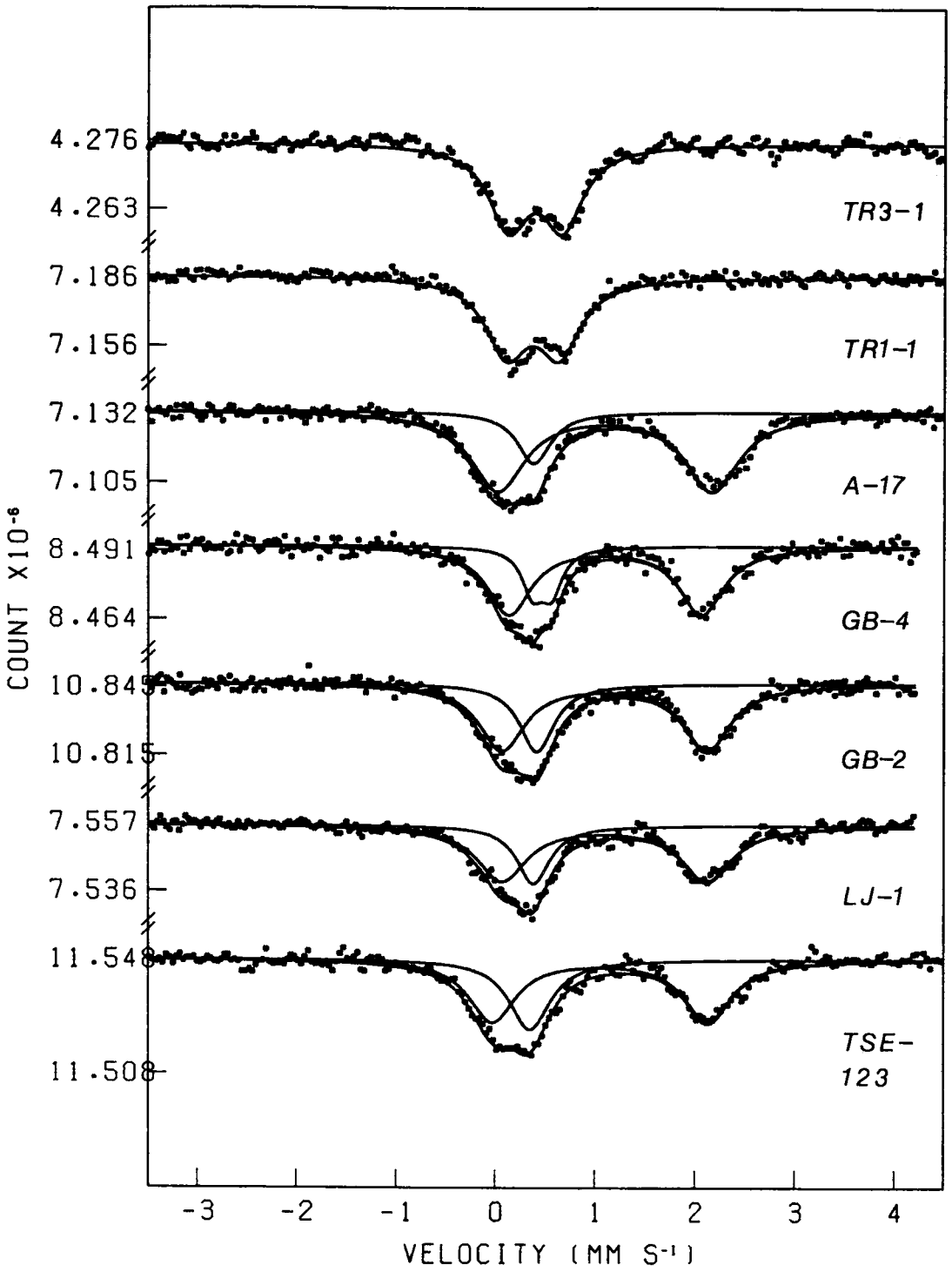
4.276
4.263
TR3-1
7.186
7.156
TR1-1
7.132
7.105
A-17
8.491
8.464
GB-4
10.845
10.815
GB-2
7.557
7.536
LJ-1
11.548
11.508
TSE-123
COUNT X10⁻⁶
-3
-2
-1
0
1
2
3
4
VELOCITY (MM S⁻¹)

TABLE 6. LITHIUM CONCENTRATION IN WODGINITE-GROUP MINERALS

Sample:	A-17	G69-23	KZ-1	LJ-3	TP-1	TSE-76	VII-1
Li (ppm):	138	275	1643	47	373	5600	87

named it lithiowodginite. In M-$LiTa_3O_8$ and lithiowodginite, Li occupies the A site, and Ta occupies the B and C sites; hence the coupled substitution Mn + Sn ⇌ Li + Ta is responsible for the incorporation of Li in the structure. Consequently, significant amounts of lithium are to be found only in Ta-rich members of the wodginite group.

To assess the range, limits and behavior of lithium in the wodginite structure, seven wodginite-group minerals were analyzed for Li by atomic absorption spectroscopy. The results are given in Table 6. Two of the samples are rich in Li; five are poor in Li. The two samples rich in Li are also enriched in Ta, which supports the mechanism of coupled substitution described above.

CRYSTALLOGRAPHY

Wodginite-group minerals typically occur as irregular aggregates of crystals or as parallel to subparallel groups of crystals. Virtually all crystals are twinned; penetration twins with {001} or {100} as the composition planes are the most common. Predominance of the form {111} in combination with this style of twinning produces a characteristic flattened bipyramidal morphology; where present,

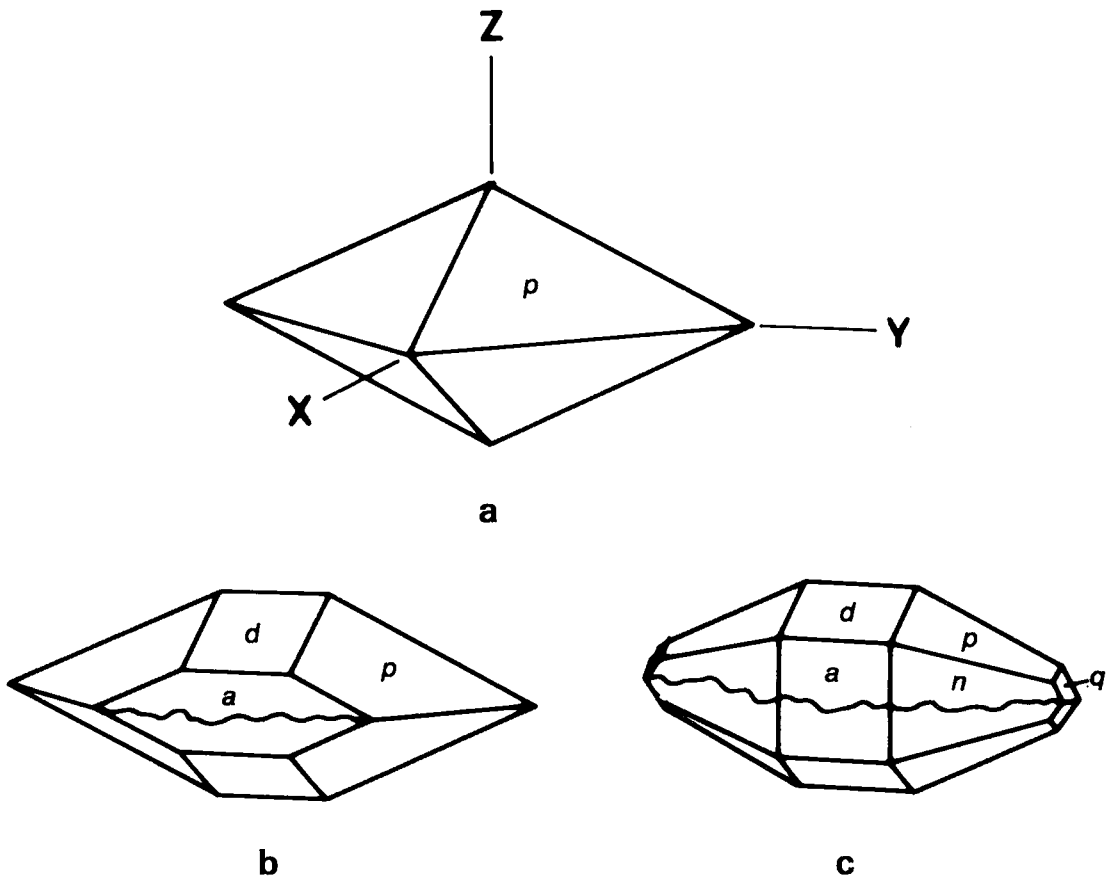

FIG. 5. The morphology of penetration-twinned wodginite-group minerals: (a) lithiowodginite, Tanco pegmatite, Manitoba; (b) ferrowodginite, Ankole, Uganda; (c) wodginite, Muhembe, Rwanda. Exaggerated irregular lines represent composition planes. Forms are a {100}, d {101}, n {310}, p {111}, q {131}.

TABLE 7. UNIT-CELL PARAMETERS FOR SPECIMENS OF WODGINITE-GROUP MINERALS

Sample	a (Å)	b (Å)	c (Å)	β (°)	V (Å³)
A-17	9.459(1)	11.427(2)	5.121(1)	90.51(2)	553.5(1)
A-25	9.466(1)	11.431(1)	5.126(1)	90.31(2)	554.6(1)
A-29	9.533(1)	11.472(1)	5.117(1)	91.17(1)	559.4(1)
A-30	9.533(2)	11.471(1)	5.117(1)	91.21(2)	559.4(1)
AC2-79-1	9.523(3)	11.476(3)	5.142(1)	90.78(3)	561.9(2)
BLM-1A	9.498(3)	11.451(3)	5.112(2)	90.99(3)	558.6(2)
G69-2	9.496(2)	11.455(2)	5.109(1)	91.07(3)	555.6(1)
G69-13	9.497(4)	11.452(4)	5.116(2)	90.94(3)	556.4(2)
G69-14	9.491(1)	11.453(1)	5.114(1)	90.95(1)	555.9(1)
G69-17	9.517(2)	11.452(3)	5.112(2)	91.10(3)	557.0(1)
G69-23	9.487(3)	11.449(2)	5.106(1)	91.04(3)	554.5(1)
G69-39	9.498(3)	11.454(2)	5.118(1)	90.93(3)	556.7(1)
G69-42	9.492(1)	11.451(1)	5.113(1)	90.97(1)	555.7(1)
G69-46A	9.492(1)	11.452(1)	5.118(1)	90.90(1)	556.2(1)
GB-1	9.468(1)	11.441(2)	5.108(1)	90.78(2)	553.2(1)
GB-2	9.480(2)	11.444(1)	5.110(1)	90.80(2)	554.3(1)
GB-3	9.506(1)	11.459(1)	5.113(1)	90.97(1)	557.0(1)
GB-4	9.469(2)	11.436(2)	5.120(3)	90.66(4)	554.4(2)
H2-1	9.472(1)	11.427(2)	5.109(1)	90.75(1)	553.0(1)
KZ-1	9.489(1)	11.491(1)	5.094(1)	91.08(1)	555.3(1)
LJ-1	9.500(1)	11.457(1)	5.138(1)	90.60(1)	559.1(1)
LJ-2	9.505(1)	11.456(1)	5.126(1)	90.82(2)	558.1(1)
MC-1	9.530(2)	11.474(1)	5.119(1)	91.14(2)	559.6(1)
MM-1	9.469(2)	11.449(3)	5.096(4)	90.83(4)	552.4(4)
OW-102	9.529(1)	11.463(1)	5.114(1)	91.20(1)	558.5(1)
SMP-12	9.520(1)	11.471(1)	5.105(1)	91.19(1)	557.4(1)
SQ-1	9.522(1)	11.467(1)	5.115(1)	91.18(2)	558.3(1)
TL-45	9.481(3)	11.444(2)	5.113(1)	90.90(3)	554.7(2)
TSE-5	9.508(2)	11.476(2)	5.102(1)	91.12(3)	556.6(1)
TSE-7	9.519(1)	11.467(1)	5.112(1)	91.21(1)	557.9(1)
TSE-16	9.486(2)	11.448(2)	5.106(1)	91.01(2)	554.4(1)
TSE-28	9.523(2)	11.477(1)	5.110(1)	91.11(2)	558.3(1)
TSE-30	9.478(1)	11.446(2)	5.116(1)	90.77(2)	555.0(1)
TSE-31	9.483(2)	11.438(2)	5.103(1)	90.91(2)	553.4(1)
TSE-32	9.489(2)	11.446(2)	5.111(1)	90.99(3)	555.0(1)
TSE-40	9.503(2)	11.458(1)	5.109(1)	91.06(2)	556.2(1)
TSE-45	9.469(2)	11.441(2)	5.108(1)	90.86(2)	553.4(1)
TSE-48	9.491(1)	11.452(1)	5.109(1)	91.03(2)	555.2(1)
TSE-65	9.480(4)	11.442(6)	5.114(2)	90.94(4)	554.7(4)
TSE-76	9.446(2)	11.504(2)	5.082(1)	91.04(2)	553.3(1)
TSE-77	9.481(2)	11.442(1)	5.116(1)	90.82(3)	555.0(1)
TSE-90	9.471(5)	11.434(2)	5.125(1)	90.40(6)	554.9(3)
TSE-97	9.483(3)	11.448(1)	5.108(1)	90.87(2)	554.5(1)
TSE-100	9.484(6)	11.441(3)	5.116(3)	90.89(9)	555.1(5)
TSE-107	9.453(2)	11.426(1)	5.097(1)	90.71(2)	550.5(1)
TSE-109	9.464(4)	11.427(3)	5.106(4)	90.62(5)	552.1(3)
TSE-122	9.417(5)	11.394(5)	5.112(2)	90.18(2)	548.5(5)
TSE-126	9.449(1)	11.418(1)	5.120(1)	90.13(3)	552.4(1)
TSE-130	9.446(3)	11.413(2)	5.115(1)	90.00(5)	551.5(1)
TSE-132	9.486(2)	11.446(1)	5.108(1)	90.93(2)	554.5(1)
TSE-134	9.462(3)	11.429(1)	5.106(1)	90.72(3)	552.1(2)
TSE-136	9.475(3)	11.441(3)	5.108(1)	90.80(3)	553.7(2)
TSE-137	9.489(2)	11.446(2)	5.121(1)	90.71(3)	556.1(1)
TSE-138	9.507(2)	11.461(1)	5.115(1)	91.05(2)	557.2(1)
TT-1	9.509(2)	11.472(1)	5.109(1)	91.14(2)	557.3(1)
VII	9.532(2)	11.466(1)	5.123(1)	91.04(2)	559.8(1)
WD-1	9.526(1)	11.474(1)	5.111(1)	91.15(1)	558.5(1)

All unit cell parameters were obtained with Philips powder diffractometers (Ni-filtered or graphite-monochromatized CuKα radiation, CaF_2 internal standard) or a Nicolet R3m single-crystal diffractometer (graphite-monochromatized MoKα radiation).

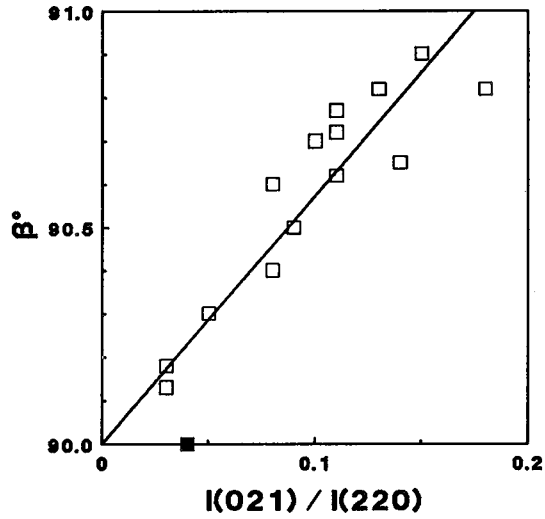

FIG. 6. Correlation of β and the relative intensity of supercell reflections; (021) is a supercell reflection, and (220) is a subcell reflection. The ratio $I(021)/I(220)$ is a measure of the relative intensity of supercell reflections. All intensities are peak heights; all intensity data were collected with a Philips PW1710 powder diffractometer using an automatic divergence slit and monochromated CuKα radiation. All samples listed in Table 12 were used in this plot, except for H2-1, which was not examined with the above model of diffractometer. The displacement of the data point shown as a filled symbol from the general trend is due to the inaccuracy of β measurement for samples in which β is approximately 90°.

this readily distinguishes wodginite-group minerals from columbite-group minerals and tapiolite (Fig. 5). Wodginite-group minerals can also be polysynthetically twinned across {100} (*e.g.* sample SK-1); however, this twin relationship is much less common than the penetration twinning.

All refined unit-cell parameters for wodginite-group minerals of this study are given in Table 7. The cell parameters show considerable variability: *a* ranges from 9.417 to 9.533 Å, *b* from 5.082 to 5.142 Å, *c* from 5.082 to 5.142 Å, and β from nearly 90° to 91.21°. We would expect from the broad chemical variations shown by wodginite-group minerals that a large part of the variation in X-ray-diffraction properties is merely symptomatic of the chemical variations. However, for a variety of wodginite compositions, the X-ray-diffraction properties of some samples (*e.g.*, A-17) are intermediate between those of ixiolite and of type wodginite. Specifically, their supercell reflections have lower relative intensities than in type wodginite, and their β angles approach 90° as the relative intensities of the supercell reflections approach 0 (Fig. 6). These features imply that wodginite-group minerals as a whole show variable degrees of order.

It is important at this stage to clarify the nature of the order–disorder phenomena. In our descriptions, we use the following terminology (Ercit *et al.* 1992b). Wodginite-group minerals that show crystallographic properties fully compatible with the ideal structure of wodginite are termed *(fully) ordered.* However, cation disorder involving mixing among the *A*, *B* and *C* sites modifies the symmetry of wodginite-group minerals, resulting in diffraction properties that are intermediate to ixiolite and wodginite; we describe these as *partially ordered.*

Order can be induced in disordered to partially ordered members of the columbite group by heating at high temperatures (Černý & Turnock 1971). On the basis of the structural and chemical similarities of columbite-group and wodginite-group minerals, it would seem likely that heating of partially ordered members of the wodginite group at conditions similar to those used for columbite-group minerals should similarly induce order.

Heating experiments were done under the same conditions standardized for columbite-group minerals by Černý & Turnock (1971), *i.e.*, 1000°C for 16 hours. Most heatings were done in air rather than in $f(O_2)$-controlled atmospheres because at the time of the experiment, all iron was assumed to be ferric on the basis of results of the synthesis work of Turnock (1966). This early oversight did not seem to introduce significant errors:

1. All heated samples were crystal fragments, not powders, minimizing the surface area available for oxidation.
2. For compositions shown by wodginite-group minerals, oxidation–reduction reactions at 1000°C are slow (Turnock 1966). Černý & Turnock (1971) showed that unit-cell dimensions of Fe-rich columbite-group minerals are statistically identical for granular samples heated in air *versus* similar samples heated in CO_2:CO controlled atmospheres. For the structural and chemical reasons outlined above, similar behavior is expected for wodginite-group minerals.
3. Most samples are Mn-rich. For these samples, oxidation of a minor proportion of iron during heating should not significantly modify patterns of order.
4. Heating experiments in atmospheres of differing $f(O_2)$ were done on the only abundant sample of a ferrous-iron-rich member of the wodginite group (A–25). A single crystal was ground to a powder and was then divided into two batches for the

TABLE 8. UNIT CELL PARAMETERS FOR HEATED SAMPLES OF WODGINITE-GROUP MINERALS

Sample	*a* (Å)	*b* (Å)	*c* (Å)	β (°)	*V* (Å³)
A-17H	9.453(1)	11.429(1)	5.098(1)	90.78(2)	550.8(1)
A-25H1	9.456(2)	11.429(2)	5.094(1)	90.86(2)	550.4(1)
A-25H2(CO)	9.457(3)	11.431(3)	5.093(1)	91.01(4)	550.5(2)
A-25H2(CO_2)	9.458(2)	11.426(2)	5.093(1)	91.04(2)	550.3(1)
A-29H	9.531(3)	11.465(2)	5.118(1)	91.22(2)	559.2(1)
A-30H	9.526(2)	11.474(2)	5.116(1)	91.19(2)	559.1(1)
AC2-79-1H	9.527(2)	11.471(2)	5.119(1)	91.15(2)	559.4(1)
G69-2H(CO)	9.492(3)	11.452(2)	5.108(2)	91.07(3)	555.1(1)
G69-2H(CO_2)	9.491(2)	11.449(2)	5.106(1)	91.06(2)	554.8(1)
G69-23H	9.485(1)	11.449(1)	5.108(1)	91.05(1)	554.6(1)
GB-2H	9.467(2)	11.434(1)	5.105(1)	90.78(2)	552.5(1)
H2-1H	9.457(2)	11.427(3)	5.098(2)	90.92(2)	550.8(2)
KZ-1H	9.484(2)	11.493(2)	5.095(1)	91.02(2)	555.3(1)
LJ-1H	9.507(1)	11.463(1)	5.116(1)	90.93(1)	557.4(1)
OW-102H	9.531(1)	11.475(1)	5.125(1)	91.12(2)	560.4(1)
TSE-7H	9.517(1)	11.469(1)	5.114(1)	91.14(2)	558.1(1)
TSE-40H	9.498(2)	11.457(2)	5.110(1)	91.11(3)	555.9(1)
TSE-45H	9.461(2)	11.432(1)	5.101(1)	91.01(2)	551.6(1)
TSE-76H	9.458(1)	11.506(1)	5.083(1)	91.04(1)	553.0(1)
TSE-126H	9.441(2)	11.414(2)	5.088(1)	90.93(2)	548.2(1)
WD-1H	9.529(2)	11.477(1)	5.121(2)	91.19(3)	560.0(2)

All heatings are in air unless otherwise indicated.

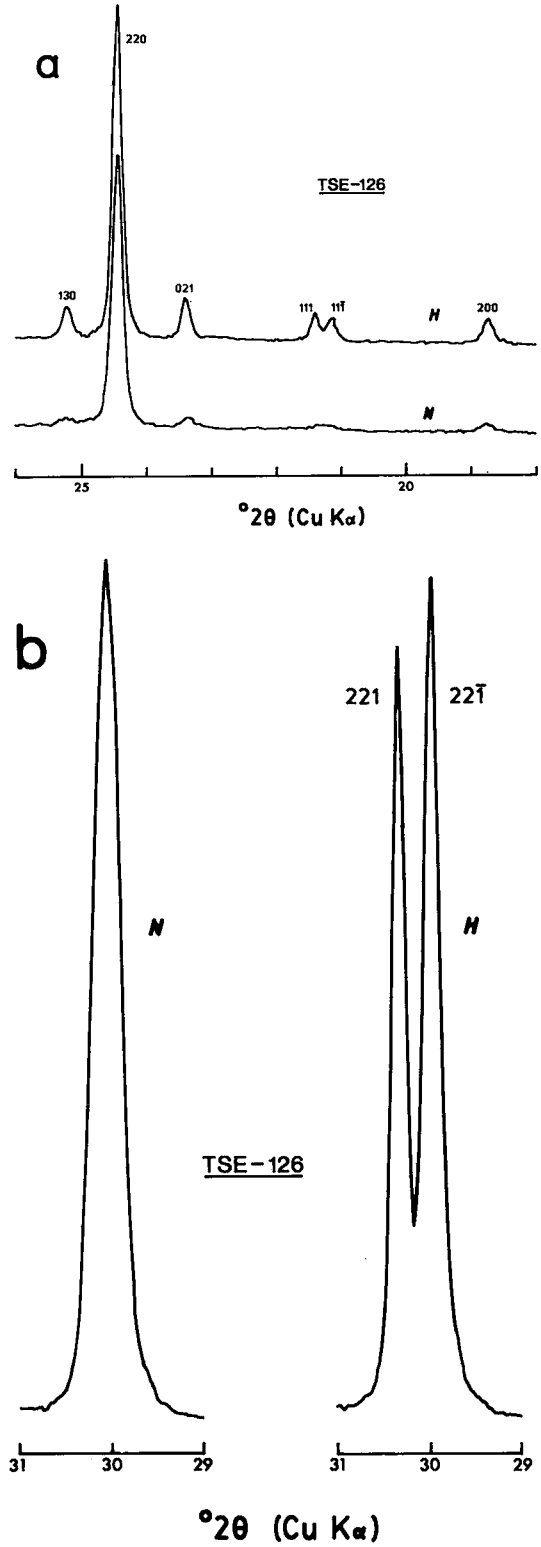

FIG. 7. Changes in X-ray powder-diffraction patterns of partially ordered members of the wodginite group with heating, as typified by sample TSE-126. (a) In the range 18° to 26° 2θ (Cu$K\alpha$), intensities of the supercell reflections (200), (11$\bar{1}$), (111), (021) and (130) increase upon heating relative to the subcell reflection (220); (b) the separation of (221) and (22$\bar{1}$) increases upon heating, indicative of an increase in β. *N*: natural, *H*: heated.

experiment. Powders were used instead of crystal fragments to ensure homogeneity and to facilitate oxidation-reduction reactions. One batch of powder was heated in CO [$f(O_2) = 10^{-17}$ atm], the other in CO_2 [$f(O_2) = 10^{-2.5}$ atm]. Heatings resulted in different colors of powder (CO_2: brown, CO: brown-black); however, no significant differences in relative peak intensities or in unit-cell parameters could be detected (Table 8, sample A-25H2), nor did extra phases form. Grice (1970) observed the same behavior for the cell parameters of samples of ordered Fe-poor wodginite.

Upon heating, many of the samples showed significantly increased intensities of supercell reflections relative to subcell reflections (Fig. 7a), increased β angles (Fig. 7b), and altered unit-cell parameters (Table 8). However, many samples failed to show significant changes upon heating. This latter group must be fully ordered; the samples that showed change upon heating must be only partially ordered.

The unit-cell parameters β and V showed the most change upon heating; they are the parameters that are most sensitive to order-disorder effects. Figure 8 is a plot of these two parameters for samples used in the heating experiments. The data for any given sample are represented as a vector (hereafter designated "heating vector"); the tail end of each vector represents the unheated sample, and the tip of each vector represents the heated sample. Most of the vectors are subparallel, and indicate that β increases and V decreases with increasing order among the cations. In two cases (WD-1 and OW-102), V was actually observed to

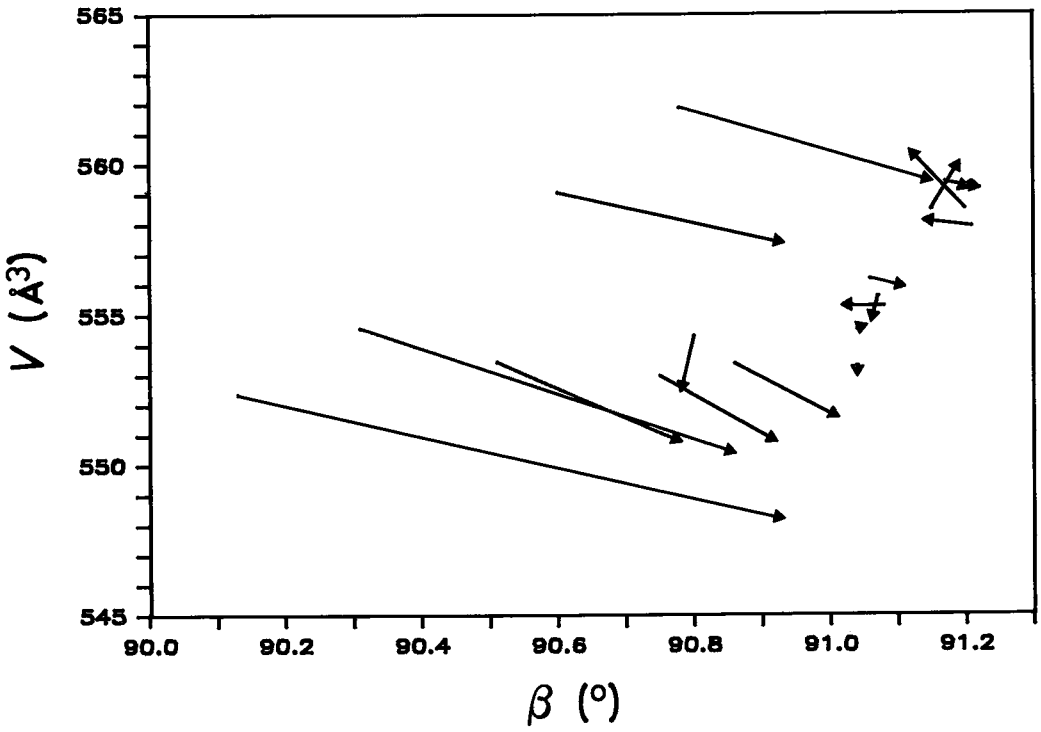

FIG. 8. Plot of unit-cell volume (V) *versus* β for natural and heated pairs of wodginite-group minerals. The tail end of each vector marks the natural sample; the tip marks the heated sample.

increase slightly upon heating, most probably owing to reaction with minor amounts of associated cassiterite detected in the patterns of the unheated but not the heated samples. The heating vectors for the Li-rich samples KZ–1 and TSE–76 slightly but significantly run opposite to the general trend. We interpret this as being due to a loss of Li during heating and not to changes in the degree of order (the relative intensities of supercell reflections for these samples do not change significantly on heating).

Formula Calculation and Site Chemistry

The calculation of formulae for wodginite-group minerals has the potential of being problematic. The majority of compositions reported in the literature were obtained by electron-microprobe analysis. Thus determinations of Fe^{2+}:Fe^{3+} ratios and Li contents are almost nonexistent. Most wodginite-group minerals are very fine grained and inhomogeneous; consequently, it is doubtful that Fe^{2+}:Fe^{3+} and Li determinations will be made in future studies unless microchemical methods are readily available. Another obstacle to calculation of a formula is the variable degree of cation order shown by wodginite-group minerals as a whole, making site assignments for individual samples impossible without some quantitative measure of the degree of order.

The initial question to be answered is whether there are sufficient constraints on the crystal chemistry of wodginite-group minerals to allow for the calculation of the two undetermined chemical variables, namely Li and Fe^{2+}:Fe^{3+}.

Chemically, the simplest site is *C*, which in fully ordered members of the wodginite group hosts only Ta and Nb. As Figure 3 and the refinement by Ferguson *et al.* (1976) show, Nb is excluded from the *B* site; it is concentrated at the *C* site, and Ta makes up the remainder of the site. On the basis of both size and charge, tungsten is expected to prefer the *C* site to the *B* site.

For fully ordered members of the wodginite group, the *B* site hosts Sn, Ti, and all Ta in excess of the *C*-site requirements. The synthesis work of Turnock (1966) shows that Fe^{3+} is localized at the *B* site. On the basis of size and charge similarities, it is expected that Sc and Zr also prefer this site.

All Mn and Li are assigned to the *A* site in fully ordered members of the wodginite group. By deduction from the work of Turnock (1966), and as Figure 2a attests, Fe^{2+} shows a strong preference for the *A* site. On the basis of arguments already presented here, Sn^{2+} is expected to prefer the *A* site.

Ignoring variable degrees of cation order for the present, the above constraints are sufficient to allow for the calculation of fully ordered formulae for wodginite-group minerals. By assigning all iron initially to the ferrous state, and iteratively adjusting the valence ratio to match *A* and *B* site-occupancies of iron, formulae were calculated for all seven samples for which Li determinations were made. The formulae for several of the samples are nonideal; their *B*- and *C*-site sums conform to wodginite stoichiometry, but their *A*-site sums are lower than expected. This is best shown by sample KZ–1; its formula is $(Mn_{0.64}Li_{0.15})_{\Sigma 0.79}(Ta_{0.65}Sn_{0.33})_{\Sigma 0.98}(Ta_{1.48}Nb_{0.52})_{\Sigma 2}O_8$, which translates to a 21% deficiency in the *A*-site sum. Such deficiencies cannot be ascribed to a systematic error in Li determination; the Li-rich sample TSE–76 shows nearly ideal stoichiometry: $(Li_{0.53}Mn_{0.43})_{\Sigma 0.96}(Ta_{0.75}Sn_{0.20}Fe^{3+}_{0.01})_{\Sigma 0.96}(Ta_{1.76}Nb_{0.24})_{\Sigma 2}O_8$.

The only possible explanation for the *A*-site deficiencies in some samples is that they represent vacancies incorporated at the site for charge-balance reasons. This is further supported by the behavior of samples KZ–1 and TSE–76 upon heating (see Crystallography), wherein heating seems to have resulted in a loss of Li from the structure without producing any significant change in diffraction properties indicative of changes in the degree of crystallinity or in the degree of cation order.

It is presumably charge imbalance at the *B* site that regulates the location and abundance of vacancies at the *A* site. The following mechanisms are responsible for balancing much of the excess positive charge introduced by *B*-site Ta:

$$2^{B}[Sn^{4+}] \rightleftharpoons {}^{B}[Fe^{3+}] + {}^{B}[Ta^{5+}]$$

$$^{A}[Mn^{2+}] + {}^{B}[Sn^{4+}] \rightleftharpoons {}^{A}[Li^{+}] + {}^{B}[Ta^{5+}]$$

Presumably, vacancies are incorporated in the wodginite structure when these mechanisms fail, *i.e.*, when μ(Li) and f(O2) are too low for the mechanisms to operate efficiently. From what has so far been established about the crystal chemistry of the wodginite group, cation-site vacancies can only be introduced if Ta^{5+} substitutes for Sn^{4+} at the *B* site; hence the incorporation of vacancies (□) at the *A* site takes place by the mechanism:

$$^{A}\square + 2^{B}[Ta^{5+}] \rightleftharpoons {}^{A}[Mn^{2+}] + 2^{B}[Sn^{4+}]$$

At first, consideration this extra complication would seem to make the calculation of ordered formulae for wodginite-group minerals a difficult task, if not an impossible one when only electron-microprobe data are available. However, Li, Fe^{2+}:Fe^{3+} and ordered-formula calculation are possible if the following constraints are applied:

1. The sum of the *B* plus *C* sites is 12 cations per unit cell.
2. All iron at the *A* site is ferrous; all iron at the *B* site is ferric. Initially all iron is assumed to be Fe^{2+}, and iron is introduced to the *B* site to meet the conditions of constraint number 1.

3. Excess positive charge introduced at the *B* site by Ta is balanced by the introduction of Fe^{3+} at the *B* site and of Li at the *A* site. As the proportion of Fe^{3+} is already dictated by constraints 1 and 2, Li can be calculated by charge-balance constraints (number of positive charges per unit cell = 64).

As a necessary consequence of the above, vacancies in cationic sites will be generated only if calculated Fe^{3+} and Li fail to balance all of the excess charge introduced by *B*-site Ta. The calculated number of Li cations represents a maximum, and the number of vacancies represents a minimum; the inherent assumption is that during growth, the wodginite structure attempts to balance excess positive charge with available cations first, and incorporates vacancies only if such cations (*i.e.*, Li, Fe^{3+}) are not available. This would seem to be responsible for the composition of sample KZ-1, which has the highest number of *A*-site vacancies to date for any member of the wodginite group, and is known to have originated in an *A*-cation-poor environment (Ercit 1986).

Using the above approach, ordered formulae were calculated for wodginite-group minerals (*e.g.*, Table 2). A FORTRAN program that facilitates the calculation of formulae is available from the Depository of Unpublished Data, CISTI, or from the senior author upon request. An important artifact of the calculations is the presence of infrequent, yet significantly low sums in the *B* site. Because the low sums do not correlate with any compositional variable, they are not inferred to be due to an unaccounted-for systematic error; consequently, they most likely indicate the presence of *B*-site vacancies. In the calculation procedure, *B*-site vacancies are produced if there are not enough pertinent cations to bring the sum of the *B* plus *C* sites to 12. There is no direct proof as to the location of the vacancies; it is inferred that the vacancies prefer the site with the lower formal charge, namely *B*. The magnitude of the largest *B*-site vacancy observed to date is 8.8%; however, as very few wodginite samples have significant numbers of *B*-site vacancies, it would seem that *B*-site vacancies play a minor role in the crystal chemistry of the wodginite group.

An indication of the correctness of the procedure for calculation of the formula comes from a comparison of measured Fe^{2+}:Fe^{3+} ratios and Li contents to respective values generated during the formula calculation. Figure 9 is a plot of calculated *versus* measured Fe^{3+}:Fe(total). Figure 10 is a plot of calculated *versus* measured Li. Agreement between observed and calculated data is very good, attesting to the validity of the procedure for calculation of the formula. The higher degree of scatter in Figure 10 may be an indication of the imprecision of Li calculation due to the large

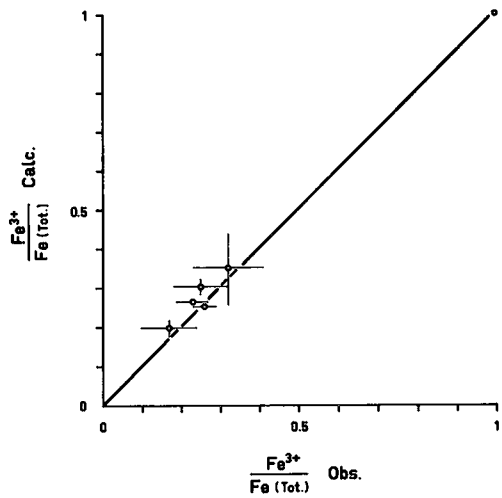

FIG. 9. Calculated *versus* observed $Fe^{3+}/(Fe^{3+}+Fe^{2+})$ for selected wodginite-group minerals. The calculated value comes from ordered formulae derived from electron-microprobe data; the observed value comes from Mössbauer experiments. The reference line marks perfect agreement between calculated and observed data.

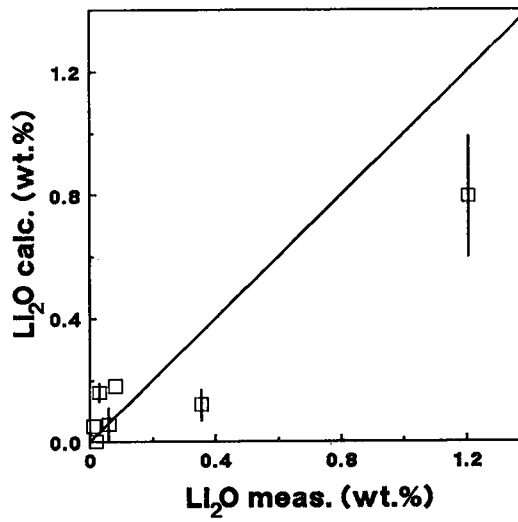

FIG. 10. Calculated *versus* observed Li_2O values for selected wodginite-group minerals. The calculated value comes from ordered formulae derived from electron-microprobe data, the observed value, from atomic absorption analysis. Vertical bars represent maximum variations in the calculation procedure due to intracrystalline zoning. The reference line marks perfect agreement between calculated and observed data.

differences in atomic weight and charge between Sn, Nb, Ta *versus* Li; *i.e.*, slight errors in the measurement of the concentrations of heavy, highly charged elements will translate into large errors in the calculation of Li^+. The vertical bars in Figure 10 represent variations in the Li calculation due solely to intracrystalline zonation; it is possible that a large component of the scatter is due also to inadequate estimation of the bulk composition from the one or two microprobe analyses used in the calculation. To be more conclusive regarding Li, more analyses of Li-rich members of the wodginite group are needed; unfortunately, known Li-rich samples are too few in number and are insufficient in bulk to allow Li determinations by conventional methods.

It should be noted that the calculation procedure concentrates vacancies at the *A* site in preference to the *B* site. The crystal-chemical reason for this approach is as follows. If vacancies are incorporated to balance excess positive charge at the *B* site, then the *A* site is the preferred locus if charge balance is to be achieved locally: in the wodginite structure (Fig. 1), there are two *A*-cation polyhedra adjacent to each *B*-cation polyhedron; however, no two *B*-cation polyhedra are mutually adjacent.

Figure 11 illustrates the variation in *A*- and *B*-site chemistry on the basis of fully ordered formulae. The chemistry of the *A* site is dominated by Mn, Fe^{2+}, Li and vacancies. In Figure 11A, data for Mn, Fe^{2+} and [Li+□] are shown; compositions of wodginite-group minerals cluster near the Mn apex, and scatter along the Mn–Fe or Mn–[Li+□] sidelines. Wodginite-group minerals with low $Mn:Fe^{2+}$ ratios tend to be impoverished in Li and *A*-site vacancies, and thus in *B*-site Ta. There is no crystal-chemical reason for such behavior. However, when this behavior is considered along with (1) sympathy between Mn and Li in pegmatitic elbaite – "tsilaisite" (Schmetzer & Bank 1984), and (2) the enrichment in Mn shown by oxide minerals in the lepidolite class of pegmatites (Černý & Ercit 1985), it seems that a common geochemical control exists for the association of Mn and Li in pegmatite minerals in general. In addition, wodginite-group minerals with high contents of Ta at the *B* site tend to form in environments characterized by high μ_{Ta} relative to the chemical potentials of other cations; these environments develop very late in pegmatite fractionation, when $Mn:Fe^{2+}$ is typically very high (Ercit 1986).

Figure 11B is a plot of the main *B*-site constituents Sn, Ti and Ta. Hollow symbols represent samples with high Fe^{3+} (>0.3 cations per unit cell), filled symbols represent samples with low Fe^{3+}. The fields for the two subgroups overlap extensively, except in the region where Ta dominates the *B*-site chemistry, a necessary consequence of the substitution mechanism $2Sn \rightarrow Fe^{3+} + Ta$. Figure 11B shows that Sn dominates in most of the compositions observed; however, natural samples never achieve end-member $MnSnTa_2O_8$ composition. As the Ti content of wodginite-group minerals decreases, the proportion of *B*-site Ta increases. This is expected to be a geochemical control; as fractionation progresses in granitic pegmatites, $\mu_{Ta}:(\mu_{Nb}+\mu_{Ti})$ typically increases, hence granitic pegmatites hosting wodginite-group minerals typically become enriched in Sn with respect to Ti prior to significant increase in the chemical potential of Ta.

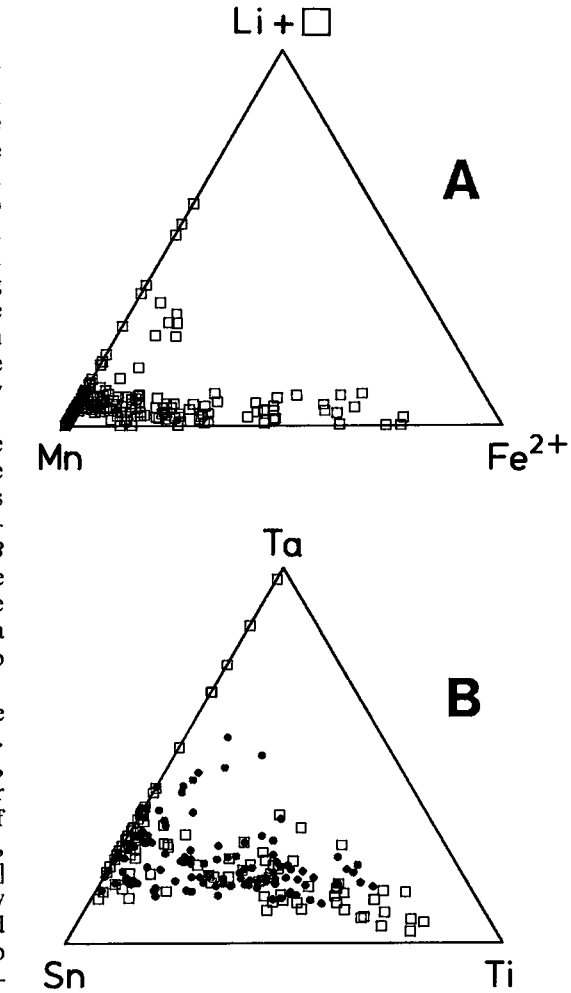

FIG. 11. Main-element chemistry of the *A* and *B* sites. For the *B*-site plot (bottom), filled symbols represent samples with Fe^{3+} less than 0.3 cations per unit cell.

The chemistry of the *C* site is not shown, as it involves only Nb-for-Ta substitutions. Concentrations of Nb in the *C* site are typically low: for the

present model of fully ordered formulae, the mean Nb occupancy is 15%, with a maximum of 35%.

Compositional – Structural Correlations

Because of the relatively large number of substitution mechanisms involved in wodginite-group minerals, coupled with the variable degrees of cation order, data on mineral chemistry and the degree of order cannot be easily derived from unit-cell parameters.

The use of heating vectors, such as in Figure 8, allows for semiquantitative assessments of the degree of order; the larger the magnitude of the vector, the less ordered the mineral is in its natural state. In Figure 8, individual heating-vectors cover a large range of the space occupied by the data; obviously, plots like this emphasize structural variability within the group. Conversely, the magnitudes of heating vectors in a–b space are less than in V–β space; a and b are relatively insensitive to cation disorder, so that a plot of a *versus* b (Fig. 12) might contain useful compositional information. This is the case; Fe- and Ti-rich compositions plot in the lower left-hand corner, Mn- and Sn-rich compositions plot in the upper parts, and compositions rich in B-site Ta (plus Li and A-site vacancies) plot closest to the lower right-hand corner of Figure 12. Concerning mineral chemistry, the low degree of scatter in Figure 12 shows that Mn ⇌ Fe and Sn ⇌ Ta isomorphism are decoupled in wodginite-group minerals: samples plot along the (Fe,Ti)-(Mn,Sn) sideline and the (Mn,Sn)-(B-site Ta) sideline, but there is no spread of data points between these sidelines. There is no crystal-chemical reason for this trend; the answer lies in pegmatite geochemistry. Extreme Ta-enrichment in granitic pegmatites tends to occur where the bulk of Mn-for-Fe substitution is nearly complete (Černý & Ercit 1985, Ercit 1986). The low degree of scatter in Figure 12 also shows that several substitutions, *e.g.*, Fe^{2+} ⇌ Mn and Ti ⇌ Sn, have similar effects upon the a and b cell parameters.

A multiple regression analysis using the SAS computer program GLM (General Linear Models) was done on 25 fully ordered synthetic, natural and heated wodginite-group minerals to assess compositional controls on unit-cell parameters. Run conditions and unit-cell parameters for the samples of synthetic wodginite are given in Table 9. The independent variables of the analysis were chosen on the basis of inferred mechanisms of substitution. The six variables used were Li, Fe^{2+}, Fe^{3+}, Ti, Nb and the sum of A- and B-site vacancies. The results of the analysis are given in Table 10; statistical information is given in Table 11. The coefficients and intercepts of the equations for each unit-cell parameter are given across each row of the table. The order of each equation was determined by stepwise addition with a maximum R^2 improvement, using the SAS program STEPWISE. With the exception of the model for β, Nb did not contribute significantly to the functions; as the presence of Nb in wodginite-group minerals is due solely to Nb-for-Ta substitution, and the effective ionic radii of Ta and Nb are identical (Shannon 1976), Nb-for-Ta substitution is not expected to affect the cell edges significantly. Five composition-

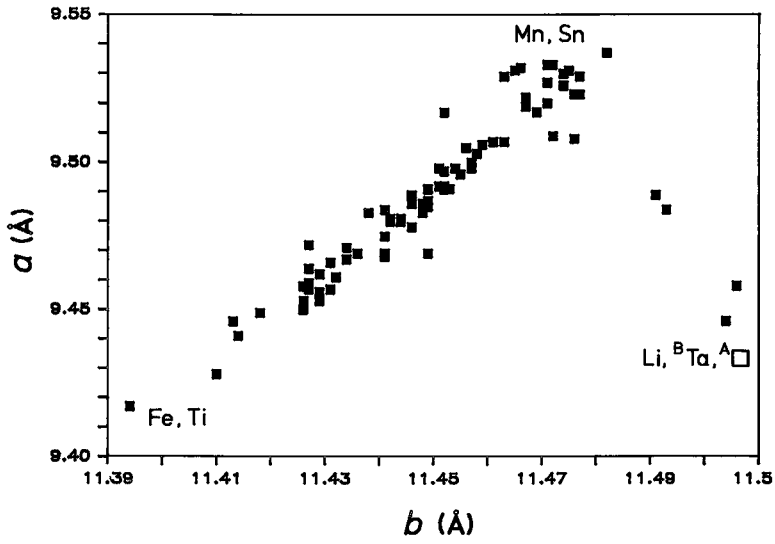

FIG. 12. Compositional trends in a–b space.

TABLE 9. SYNTHETIC WODGINITE-GROUP PHASES USED IN CELL PARAMETER CALCULATIONS

Composition	Starting Mixture	T (°C)	Medium	Run Time (h)
$MnSnTa_2O_8$	$MnCO_3 + SnO_2 + Ta_2O_5$	1050	air, 1 atm	10+10
$MnTiTa_2O_8$	$MnCO_3 + TiO_2 + Ta_2O_5$	1050	air, 1 atm	10+10
$Mn_2Fe^{3+}Ta_5O_{16}$	$2MnTa_2O_6 + FeTaO_4$	1225	air, 1 atm*	

	CELL PARAMETERS		
	$MnSnTa_2O_8$	$MnTiTa_2O_8$	$Mn_2Fe^{3+}Ta_5O_{16}$
a	9.537(1) Å	9.428(2) Å	9.450(1) Å
b	11.482(1)	11.410(1)	11.426(1)
c	5.124(1)	5.084(1)	5.094(1)
β	91.24(1) °	91.20(1) °	90.89(1) °
V	561.0(1) Å^3	546.7(1) Å^3	549.7(1) Å^3

* from Turnock (1966).

TABLE 10. RESULTS OF THE MULTIPLE REGRESSION ANALYSIS

Cell Parameter	Intercept	Coefficients						R^2 (%)
		Fe^{2+}	*Li*	□	*Ti*	Fe^{3+}	*Nb*	
a	9.539	-0.014	-0.034	-0.032	-0.031	-0.044	0	95
b	11.475	-0.008	0.012	0	-0.019	-0.028	0	94
c	5.123	0	-0.017	-0.024	-0.011	-0.014	0	93
β	91.28	-0.10	-0.04	0	-0.03	-0.21	-0.11	91
V	560.5	-1.5	-3.2	-4	-3.8	-5.3	0	93

Units: *a*, *b*, *c*: Å; β: °; *V*: Å^3.

TABLE 11. STATISTICAL DATA FOR TABLE 10

	Intercept	Fe^{2+}	*Li*	□	*Ti*	Fe^{3+}	*Nb*
a	5(0.0)	4(0.3)	2(0.0)	10(0.5)	2(0.0)	6(0.0)	-
b	2(0.0)	3(1.9)	2(0.0)	-	2(0.0)	4(0.0)	-
c	2(0.0)	-	1(0.0)	5(0.0)	1(0.0)	3(0.0)	-
β	2(0.0)	2(0.0)	1(0.1)	-	1(0.3)	2(0.0)	2(0.0)
V	6(0.0)	5(1.2)	3(0.0)	1(0.4)	3(0.0)	7(0.0)	-

Leading numbers are standard deviations on the last significant figure of the corresponding parameters of Table 10. Numbers in parentheses are % probabilities for $H_0|t|=0$.

al variables were necessary to model *a*, β and *V*; only four were needed to model *b* and *c*. Because of the way the variables were selected, the intercepts of the five equations necessarily represent the cell parameters of $MnSnTa_2O_8$. Input to the equations consists of the number of atoms per unit cell of each independent variable, based on the calculations of the fully ordered formulae. As an example, the calculated *a* cell edge of hypothetical $FeTiTa_2O_8$ would be 9.539 - (0.014 * 4) - (0.031 * 4) = 9.359 Å.

Problems with the set of calibration data and regression model are not trivial:

1. Powder-diffraction data represent structural data for a bulk sample; estimation of the bulk composition of the sample from electron-microprobe data is difficult owing to strong compositional zoning of some samples. In cases where core and rim compositions of a crystal are available, the assigned bulk composition is taken to be a weighted mean of 2/3 times the core composition plus 1/3 of the rim composition.
2. In nearly all cases, separate parts of crystals or separate batches of crystals were used for microprobe analysis *versus* powder diffractometry. As such, the bulk compositions of the powders may deviate significantly from the microprobe-derived composition.
3. The multiple regression model is a linear one, whereas solid solution in minerals may result in nonlinear correspondence between compositional data and unit-cell parameters (Newton & Wood 1980).

Despite the above considerations, the equations of Table 10 predict the unit-cell parameters of wodginite-group minerals reasonably precisely; the root mean square (RMS) errors in *a*, *b* and *c* are 0.009, 0.007 and 0.004 Å respectively, in β the RMS is 0.04° (comparable to the precision of β measurement from precession photographs), and in *V* it is 1.2 Å^3. Figure 13 shows the correspondence between observed and calculated values of *a*, *b*, *c* and β. The low degree of scatter of the data and lack of any systematic deviation from ideality for any of the three types of sample (natural, heated and synthetic) further attest to the validity of the calculation procedure.

With the data of Table 10, unit-cell parameters can be calculated from the fully ordered formulae of wodginite-group minerals; the result of such a calculation necessarily gives cell parameters devoid of the effects of cation disorder, *i.e.*, comparable to the cell parameters of heated wodginite-group minerals. The advantage of such a calculation is that information on degree of cation order in wodginite-group minerals can be obtained without having to resort to heating experiments, which is especially useful where samples are inhomogeneous.

The β angle is best to quantify the degree of order, as the sensitivity of β to disorder has already been established, and unlike the other cell parameters, the value of β for fully disordered wodginite (= ixiolite, *sensu stricto*) is known (90°). An *index of order* (Δ) for wodginite-group minerals, defined as $[\beta(\text{obs}) - 90°]/[\beta(\text{ord}) - 90°]$, should serve as a measure of the degree of order of the sample. β(obs) refers to the unheated sample, and β(ord), to either β calculated from Table 10 or obtained from heating experiments. Samples for which Δ is equal to 0 are fully disordered, samples with Δ equal to 1 are fully ordered, and samples with intermediate values of Δ are partially ordered. On the basis of the precision of measurement and calculation of β, the relative standard deviation associated with the calculation of Δ is estimated to be 5%.

The assumption inherent in this approach is that the transformation from ixiolite to wodginite is continuous, *i.e.*, the relationship between Δ and the degree of order is taken to be continuous and linear. The possibility of the transformation being

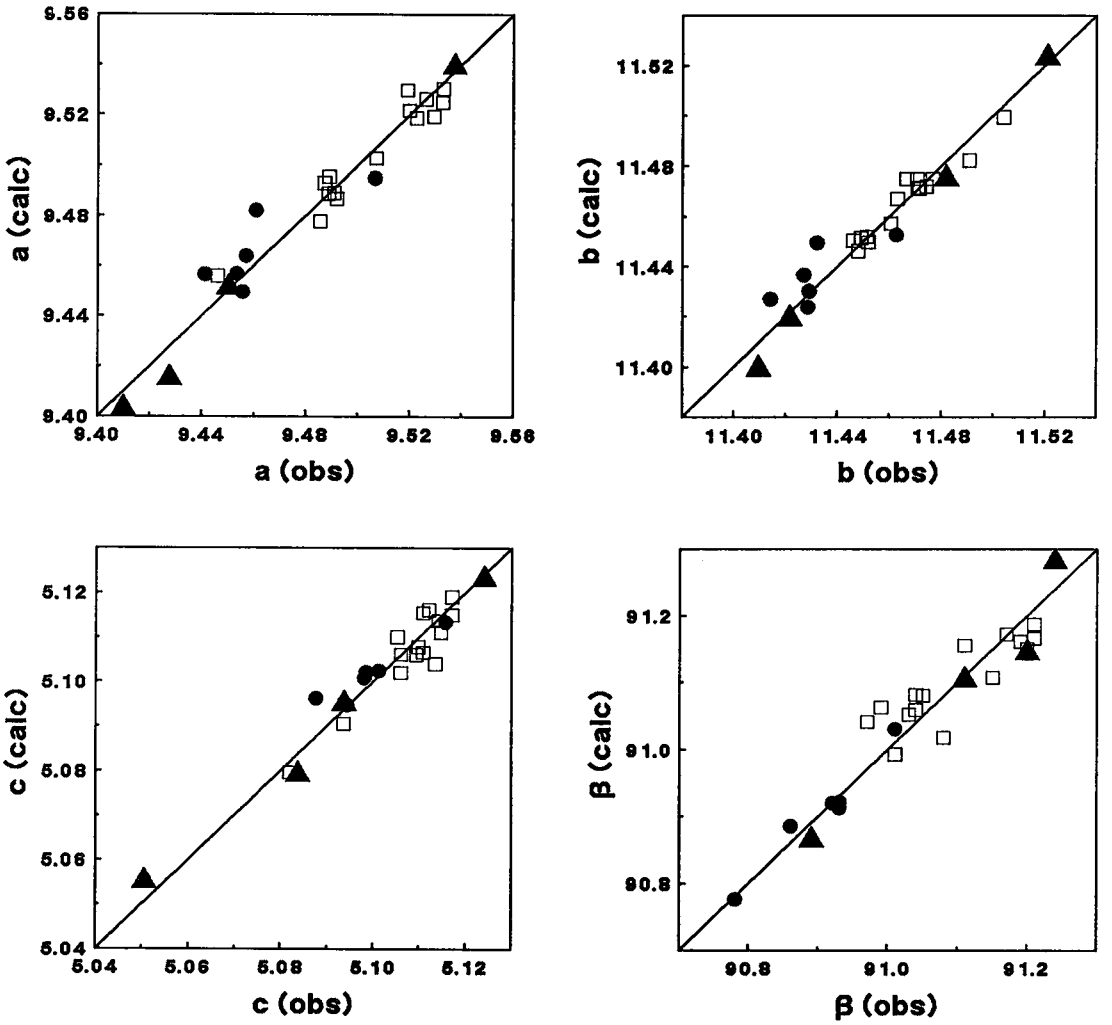

FIG. 13. Plots of calculated *versus* observed unit-cell parameters (a, b, c, β) for samples used in the regression analysis. Squares denote natural samples, filled circles denote heated samples, and filled triangles denote synthetic wodginite.

discontinuous cannot be ruled out; however, plots like Figure 6 suggest that at the current level of precision, the assumption of a continuous transformation is probably acceptable.

Estimates of the degree of order for selected wodginite-group minerals are given in Table 12. The validity of the definition of the ordering index is shown by the excellent agreement between Δ(calc) from Table 12 and Δ(meas) from the structural study (Ercit *et al.* 1992b) for the partially ordered samples CX-1 and A-17. Sample CX-1, Ta-rich wodginite, has a Δ(calc) of 0.60 and a Δ(meas) of 0.59(1); sample A-17, Fe^{2+}-rich wodginite, has a Δ(calc) of 0.65 and a Δ(meas) of 0.66(1). Furthermore, all samples from the structural study

TABLE 12. DEGREE OF ORDER FOR SELECTED SAMPLES OF WODGINITE-GROUP MINERALS

Sample	β(obs)°	β(calc)°	Δ	% Order*
TSE-130	90.00	90.90	0.00	0
TSE-126	90.13	90.92	0.14	15
TSE-122	90.18	90.87	0.21	20
A-25	90.31	90.88	0.35	35
TSE-90	90.40	90.93	0.43	45
TSE-109	90.62	90.99	0.63	65
A-17	90.51	90.78	0.65	65
LJ-1	90.60	90.91	0.66	65
TSE-137	90.71	91.07	0.66	65
TSE-134	90.72	91.00	0.72	70
GB-4	90.66	90.86	0.77	75
TSE-30	90.77	90.97	0.79	80
TSE-77	90.82	91.01	0.81	80
H2-1	90.75	90.93	0.81	80
G69-46a	90.90	91.02	0.88	90
LJ-2	90.82	90.88	0.93	95
G69-17	91.10	91.14	0.96	95

* rounded to the nearest 5% .

that were inferred to be fully ordered have calculated values of Δ statistically identical to 1.

SUMMARY

1. Wodginite, *sensu stricto*, has the general formula ABC_2O_8, where A = Mn, B = Sn^{4+}, C = Ta.
2. Other cation constituents (minor ones in parentheses) are: A site: Fe^{2+}, Li, (Sn^{2+}, Ca); B site: Ti, Fe^{3+}, Ta, (Sc, Zr); C site: Ta, Nb, (W).
3. Vacancies occur at the A cation site and seem likely for the B site.
4. Taking the site preferences of Fe^{2+} (A site) *versus* Fe^{3+} (B site) into consideration, cation-ordered formulae can be calculated for wodginite-group minerals. As a consequence of the formula-calculation procedure, Fe^{2+}:Fe^{3+} and the Li contents can be calculated.
5. Multiple-regression analysis of compositional and structural data has resulted in a set of equations with which unit-cell parameters can be calculated from compositional data. The equations necessarily give parameters that pertain to the fully ordered state.
6. Natural members of the wodginite group are commonly only partially ordered. The degree of cation order can be assessed qualitatively by examination of the ratio $I(021)/I(220)$, or the value of the β angle or unit-cell volume. The degree of cation order can be quantified by (1) crystal-structure refinement, (2) comparison of the β angles of natural samples with their heated counterparts, (3) comparison of measured unit-cell parameters (especially β) for natural samples with the parameters calculated from the equations described above (point 5).

ACKNOWLEDGEMENTS

The authors thank A.J. Anderson, E.E. Foord, A.-M. Fransolet, R.V. Gaines, R.I. Gait, O. von Knorring, R. Kristiansen, S. Lahti, J. Luna, I. Nakai, Ni Yung Xiang, the late W.L. Roberts, the late T.G. Sahama, R. Schooner, J. Siivola, A.C. Turnock, A.V. Voloshin, S. White and M.A. Wise for the loan of samples. E.E. Foord generously supplied information about Sn^{2+} in wodginite. We are indebted to the Tantalum Mining Corporation of Canada Limited for access to the workings of the Tanco pegmatite during the period of study, and to Tanco mine geologists R.A. Crouse and P. Vanstone for their help with our underground activities. Financial support for the study was in the form of a NSERC operating grant, DEMR Research Agreement, and Tantalum Mining Corporation of Canada contract to PČ, a NSERC operating grant to FCH, and a NSERC Postgraduate Scholarship, University of Manitoba fellowships to TSE and a Canadian Museum of Nature research stipend to TSE. We appreciate the careful editing by R.F. Martin.

REFERENCES

APPLEMAN, D.E. & EVANS, H.T., JR. (1973): Job 9214: indexing and least-squares refinement of powder diffraction data. *U.S. Geol. Surv., Comput. Contrib.* **20** (*NTIS Doc.* **PB2-16188**).

ČERNÝ, P. & ERCIT, T.S. (1985): Some recent advances in the mineralogy and geochemistry of Nb and Ta in rare-element granitic pegmatites. *Bull. Minéral.* **108**, 499-532.

_____ & _____ (1990): Mineralogy of niobium and tantalum: crystal chemical relationships, paragenetic aspects and their economic implications. *In* Lanthanides, Tantalum and Niobium (P. Möller, P. Černý & F. Saupé, eds.). Springer-Verlag, Berlin (27-79).

_____ & TURNOCK, A.C. (1971): Niobium–tantalum minerals from granitic pegmatites at Greer Lake, southeastern Manitoba. *Can. Mineral.* **10**, 755-772.

COLBY, J.W. (1980): MAGIC V – a computer program for quantitative electron-excited energy dispersive analysis. *In* QUANTEX-Ray Instruction Manual. Kevex Corporation, Foster City, California.

ERCIT, T.S. (1986): *The Simpsonite Paragenesis. The Crystal Chemistry and Geochemistry of Extreme Ta Fractionation.* Ph.D. thesis, Univ. Manitoba, Winnipeg.

_____, ČERNÝ, P. & HAWTHORNE, F.C. (1992a): The wodginite group. III. Classification and new species. *Can. Mineral.* **30**, 633-638.

_____, _____ & SIIVOLA, J. (1987): The composition of stannomicrolite. *Neues Jahrb. Mineral. Monatsh.*, 249-252.

_____, HAWTHORNE, F.C. & ČERNÝ, P. (1992b): The wodginite group. I. Structural crystallography. *Can. Mineral.* **30**, 597-611.

FERGUSON, R.B., HAWTHORNE, F.C. & GRICE, J.D. (1976): The crystal structures of tantalite, ixiolite and wodginite from Bernic Lake, Manitoba. II. Wodginite. *Can. Mineral.* **14**, 550-560.

GATEHOUSE, B.M., NEGAS, T. & ROTH, R.S. (1976): The crystal structure of *M*–$LiTa_3O_8$ and its relationship to the mineral wodginite. *J. Solid State Chem.* **18**, 1-7.

GRICE, J.D. (1970): *The Nature and Distribution of the Tantalum Minerals in the Tanco Mine Pegmatite at Bernic Lake, Manitoba.* M.Sc. thesis, Univ. Manitoba, Winnipeg, Manitoba.

KOMKOV, A.I. (1970): Relationship between the X-ray

constants of columbites and composition. *Dokl. Acad. Sci. USSR* **195**, 117-119.

_____ & DUBIK, O. YU. (1983): Chemical composition of wodginites and possible conditions of their formation in nature. *In* Problemy Kristallokhimii i Genezisa Mineralov (A.V. Sidorenko & D.V. Rundkvist, eds.). Izdatel'stvo Nauka, Leningrad (124-129; in Russ.).

LONG, G.L., CRANSHAW, T.E. & LONGWORTH, G. (1983): The ideal Mössbauer effect absorber thicknesses. *Mössbauer Effect Ref. Data J.* **6**, 42-49.

MAKSIMOVA, N.V. & KHVOSTOVA, V.A. (1970): Mineralogy and crystal chemistry of some tantaloniobates. *Dokl. Acad. Sci. USSR* **193**, 119-122.

NEWTON, R.C. & WOOD, B.J. (1980): Volume behavior of silicate solid solutions. *Am. Mineral.* **65**, 733-745.

SCHMETZER, K. & BANK, H. (1984): Crystal chemistry of tsilaisite (manganese tourmaline) from Zambia. *Neues Jarhb. Mineral. Monatsh.*, 61-69.

SHANNON, R.D. (1976): Revised effective ionic radii and systematic studies of interatomic distances in halides and chalcogenides. *Acta Crystallogr.* **A32**, 751-767.

SIDORENKO, G.S., SOLNTSEVA, L.S. & GORZHEVSKAYA, S.A. (1974): Minerals with wodginite structure and their synthetic analogues. *Dokl. Acad. Sci. USSR* **216**, 127-130.

TURNOCK, A.C. (1966): Synthethic wodginite, tapiolite and tantalite. *Can. Mineral.* **8**, 461-470.

VOLOSHIN, A.V., PAKHOMOVSKII, YA.A. & BAKHCHISARAITSEV, A.YU. (1990): Lithiowodginite – a new mineral of the wodginite group from granitic pegmatites in eastern Kazakhstan. *Mineral. Zh.* **12**, 94-100 (in Russ.).

Received June 26, 1991, revised manuscript accepted May 21, 1992.